Paul Salzmann, BSc

Preparation of smart thermo-responsive polymer thin films by initiated chemical vapor deposition

MASTER'S THESIS

to achieve the university degree of

Diplom-Ingenieur

Master's degree programme: Technical Physics

submitted to

Graz University of Technology

Supervisor

Ass.Prof. Dr. Anna Maria Coclite

Co-supervisor
Univ.-Prof. Ph.D. Peter Hadley

Institute of Solid State Physics

Graz, March 2017

AFFIDAVIT

I declare that I have authored this thesis independently, that I have not used other than the declared sources/resources, and that I have explicitly indicated all material which has been quoted either literally or by content from the sources used. The text document uploaded to TUGRAZonline is identical to the present master‘s thesis.

Date

Signature

Acknowledgement

First I would like to thank my supervisor Anna Maria Coclite for supporting and teaching me during my time working on this thesis. She guided me through my work, motivated me and had always time for me if I needed a piece of advice. I also want to express my gratitude to my co-supervisor Peter Hadley for his input and his help with finding suitable substrates.

Special thanks go to Paul Christian who always took his time to help me in the lab and for his constructive discussions and input. Furthermore I want to thank Katrin Unger for her help with my first depositions. I also thank the whole CVD-ALD group including Martin Tazreiter, Julian Pilz, Stephan Tumphart and Marianne Kräuter for their input and friendly working atmosphere.

Here I also want to acknowledge Andreas Hohenau for his kind support with the surface plasmon resonance spectroscopy experiments we did at University of Graz.

I also would like to thank Roland Resel and his group for the constructive discussions and interesting talks we had during our group meetings. The help of Birgit Kunert, Elisabeth Stern, Harald Kerschbaumer is appreciated.

Last but no least I would like to thank my parents Martina and Gerhard Salzmann as well as Lena Hirschenberger for their never ending support during all my student life.

Abstract

Stimuli-responsive polymers, like the thermo-responsive Poly-(N-Isopropylacrylamide), short p(NIPAAm), show high response to small changes in their environment (e.g. temperature, pH or humidity changes), which makes them suitable for nanotechnology or nanomedicine (e.g. drug delivery, artificial muscles).
In the case of the studied p(NIPAAm), changes of temperature trigger changes in thickness of polymer thin films in aqueous solution. This arises from a coil to globule transition from a swollen hydrophilic state at temperatures below the lower critical solution temperature (LCST) to a shrunken hydrophobic state when the material is heated to temperatures higher than the LCST. Copolymer thin films of NIPAAm cross-linked with Di(ethylene glycol) divinyl ether (DEGDVE) were synthesized by initiated chemical vapour deposition (iCVD) and studied regarding their behaviour when exposed to water and water vapor. It was found that film thicknesses were up to three times higher at lower temperatures below the LCST than in the hydrophobic state at higher temperatures. In order to shift the LCST, different monomers were used. By copolymerizing N,N-Diethylacrylamide (DEAAm) with DEGDVE response at higher temperatures could be measured. The prepared films were investigated by Fourier transform infrared spectroscopy, spectroscopic ellipsometry and surface plasmon resonance spectroscopy.

Kurzfassung

Stimuli-responsive Polymere, wie das untersuchte auf Temperaturänderungen reagierende Poly-(N-Isopropylacrylamid), kurz p(NIPAAm), zeigen starke Reaktionen auf kleine Veränderungen in ihrer Umgebung (Temperatur, pH-Wert, Luftfeuchtigkeit). Diese Eigenschaft macht diese Materialien anwendbar in Bereichen der Nanotechnologie (z.B. Sensoren, funktionelle Beschichtungen) oder Nanomedizin (z.B. gezielt lokale Medikamentenfreisetzung im Körper, künstliche Muskeln).
Das in dieser Arbeit untersuchte Polymer p(NIPAAm), als Dünnschicht synthetisiert, reagiert bei Temperaturänderungen mit einer Veränderung der Schichtdicke in wässriger Lösung. Der Grund für diese Eigenschaft ist jene, dass das Material einen Phasenübergang von einem hydrophilen Zustand unter der unteren kritischen Lösungstemperatur (LCST) zu einem hydrophoben Zustand oberhalb dieser besitzt. In wässriger Lösung nimmt das Polymer, wenn es sich im hydrophilen Zustand unter der kritischen Lösungstemperatur befindet, Wasser aus seiner Umgebung auf, was zu einer Zunahme der Schichtdicke eines Polymer-Dünnfilms führt.
Zur Untersuchung dieser Eigenschaften in flüssigem Wasser und unter Bedingungen mit hoher Luftfeuchtigkeit wurden Copolymer-Dünnfilme aus NIPAAm, vernetzt mit Di(ethyl glycol) divinyl ether (DEGDVE), mittels initiierter chemischer Gasphasenabscheidung (Englisch: initiated Chemical Vapor Deposition, iCVD) synthetisiert.
Es konnte gezeigt werden, dass die Schichtdicke der Filme bei Temperaturen unter der kritischen Lösungstemperatur auf das bis zu Dreifache anwuchs, im Vergleich zu wenn die Temperatur höher als die LCST war.
Durch die Verwendung eines anderen Monomers, N,N-Diethylacrylamid (DEAAm), copolymerisiert mit DEGDVE konnte eine Verschiebung der unteren kritis-

chen Lösungstemperatur erreicht werden. Für diese Filme wurden Schichtdickenänderungen bei höheren Temperaturen gefunden.
Die hergestellten Polymer-Dünnfilme wurden mit Fourier-Transformations-Infrarotspektroskopie, spektroskopischer Ellipsometrie und Oberflächenplasmonenspektroskopie untersucht.

Contents

CHAPTER 1

Introduction and Motivation

Smart or stimuli-responsive polymers react to changes in their environment (e.g. temperature or humidity). For instance, the thermo-responsive polymer poly(N-Isopropylacrylamide), p(NIPAAm), undergoes a reversible coil-to-globule transition in aqueous solution at a certain temperature. Effects like this can be used in various applications, like nanotechnology or nanomedicine. Stefano Palagi et al. show in [18] that they were able to build a swimming micro-robot, based on light-responsive polymers. The material shrinks when exposed to light, which is used to trigger a peristaltic movement, by illuminating the robot in an ordered pattern, as it is shown in figure 1.1.

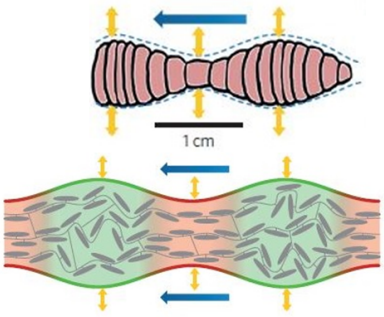

Figure 1.1: Peristaltic movement, induced by local changes of thickness due to patterned illumination of the sample. Reprinted from[18].

An other possible application of simuli-responsive polymers would be sen-

sors, based on polymers which are responsive to the quantity one wants to measure. In the ERC Starting Grant project "Smart Core" the goal is to measure local changes of temperature and humidity (see fig. 1.2). The polymer p(NIPAAm) is a possible candidate for the smart sensing material, as it undergoes a reversible coil-to-globule tranisition from a hydrophobic state below its lower critical solution temperature (LCST) at 32 °C to a hydrophobic state above it[1]. The idea is, to have stimuli-responsive nano-rods, encapsulated with piezoelectric zinc-oxide in order to transform the signal coming from the polymers to a measurable voltage pulse (see [7]). By arranging these elements in an array, one would be able to detect local changes in e.g. temperature.

Summarizing all this, the aim of this work was to synthesize polymer thin

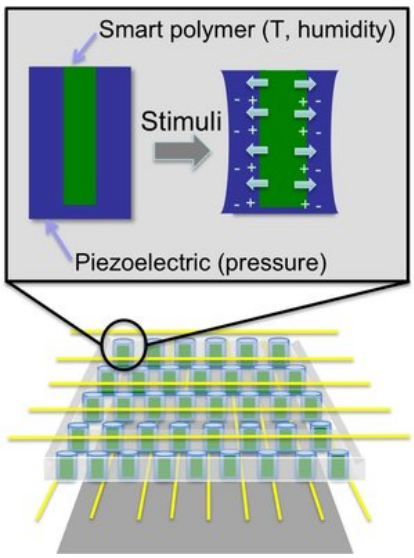

Figure 1.2: Smart polymer nanorods, encapsulated with piezoelectric ZnO will be arranged in an array, to be able to measure local changes in e.g. temperature and humidity. Reprinted from [7].

films, which show high swelling in water in the first place and furthermore show response to changes in temperature.

CHAPTER 2

Fundamentals

2.1 Polymers

2.1.1 Polymer basics

Polymers are long, chain-like molecules which are built from a repeat unit, called a monomer. The process of forming polymers is called polymerization. In our every day life, we come across different kind of natural polymers like cellulose in wood, DNA or natural rubber and synthethic polymers like nylon, neoprene or synthetic rubber. The individual monomers or building blocks are connected via covalent bonds and can usually rotate to the bonding axis, leading to a high number of internal degrees of freedom of the polymer chains and therefore an enourmous number of spatial conformations [8]. The organic backbone of a polymer consists mainly of carbon atoms. The high molecular mass of polymers leads to unique physical properties like viscoelasticity or toughness. If a polymer only contains one kind of monomer it is called homopolymer and if there are more than one repeat unit present in the polymer it is called a copolymer.
A simple example for a polymer is polypropylene which one can see in fig. 2.1.

A more complex polymer is poly-N-Isoproplyacrolamide, which was synthesized in this work and can be seen in fig. 2.2. The C=C double bond in fig. 2.2b is the site where the monomer polymerizes and attaches to the carbon backbone.

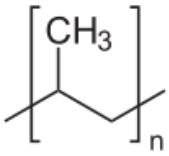

(a) Chemical structure of polypropylene

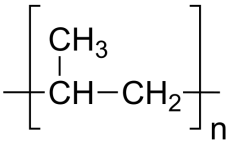

(b) Repeating unit of polypropylene

Figure 2.1: Chemical structure of polypropylene and it's repeating unit.

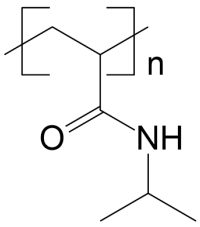

(a) Chemical structure of p(NIPAAm)

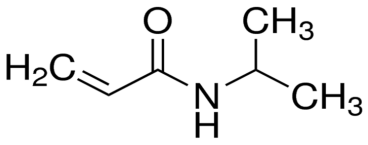

(b) Chemical structure of the monomer NIPAAm. The polymerization takes place at the C=C double bond.

Figure 2.2: Chemical structure of the polymer p(NIPAAm) and its repeating unit

2.1.2 Copolymers

A copolymer is a polymer containing at least two different repeating units. The different monomers can arrange in different ways along the chain, which are shown in figure 2.3. The first case (1) in fig. 2.3 illustrates a homopolymer with a single monomer A. Now we consider two different subunits A and B. Alternating copolymers form a structure where the units A and B are regularly alternating (2). When the monomers arrange in a random manner, the polymer is considered a random copolymer, which is drawn in (3). The structure (4) describes the case where two or more homopolymer subunits are covalently bound together and form a so called block-polymer. In iCVD, two types of copolymerization have been observed, namely alternating copolymerization and random copolymerization [9].

Figure 2.3: Different types of copolymers.

Copolymerization can be used to tune the polymer properties. By incorporating a crosslinker into the copolymer, the mechanical properties can be enhanced. A network of hydrophilic polymer chains connected to each other via crosslinker units is called a hydrogel. The degree of swelling of such a hydrogel is closely related with the degeree of crosslinking. With increasing degree of crosslinking, hydrogels swell less, because the polymer chains are linked more tightly. [9]

2.1.3 Mesh size

A characteristic quantity regarding crosslinked polymer networks is the mesh size. It is the length scale of two sequential crosslinks in the polymer matrix. The Flory-Rehner theory links the mesh size of a polymer chain network with it's swelling in water in thermodynamic equilibrium. From swelling experiments one can determine the the average molecular weight between two cross-links $\overline{M_c}$, which can be calculated like the following [21]:

$$\frac{1}{\overline{M_c}} = -\frac{2}{M_m}\frac{ln\left(1-\frac{d_0}{d}\right)+\frac{d_0}{d}+\chi\left(\frac{d_0}{d}\right)^2}{2\frac{d}{d_0}-\frac{d_0}{d}} \tag{2.1}$$

with d_0 is the initial thickness in dry stage, d the thickness of the swollen film in liquid water. M_m is the molecular weight of the monomer. The interaction parameter χ for NIPAAm and water can be found in literature [11].
In order to calculate the mesh size, one can use the following formula[21]:

$$\xi = \left(\frac{d_0}{d}\right)^{-\frac{1}{3}} l\left(\frac{2\overline{M_c}}{M_m}\right) \tag{2.2}$$

2.2 Lower critical solution temperature (LCST)

The lower critical solution temperature is the temperature, below which all components of a system mix in all proportions and above which they form two separate phases. [3]. Polymers that undergo a LCST transition in water are soluble at low temperatures and separate at temperatures higher the LCST. Thermodynamically this means that the change of the Gibbs free energy (see eq. 2.3) for dissolving in water is negative at low temperatures and becomes positive for high temperatures.

$$\Delta G = \Delta H - T\Delta S \tag{2.3}$$

This is possible when the enthalpy for dissolution ΔH is negative, which can come from hydrogen bonds between water molecules and polymer chains. The entropy contribution ΔS for this case is then negative too, as there is a loss in entropy for water molecules binding to the polymer chains. When the temperature is increased, the enthalpic hydrogen bonding interaction decreases and the entropy term $-T\Delta S$ becomes dominant, leading to a positive Gibbs free energy ΔG of mixing, resulting in a phase separation . This means that water molecules go back to the bulk water leaving the collapsed polymer chains behind. This transition from a hydrated to a dehydrated state is fully reversible. The LCST strongly depends on the polymer structure as polymers with more hydrophilic structure show a higher LCST. [12]

2.2.1 NIPAAm: Coil-to-globule transition

In the case of the studied polymer N-Isopropylacrylamide (p(NIPAAm)), the polymer exhibits a LCST transition at 32 °C [1]. During the transition the polymer restructures in a kind that the hydrophilic groups which are pointed outwards below the LCST rearrange by intra-molecular hydrogen bonds, in a form that the hydrophobic groups are exposed to the polymer's surface.

The described LCST transition leads to a coil-to-globule transition from a swollen hydrated phase below the LCST to a shrunken, hydrophobic state above, when in aqueous solution.

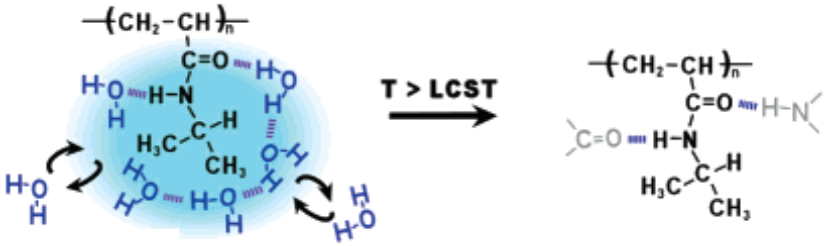

Figure 2.4: Water molecules bonded via hydrogen bonds to the functional groups of p(NIPAAm) (left). At elevated temperatures above the LCST, the functional groups rearrange with forming hydrogen bonds between each other (right). This leads to a hydrophobic state where the water molecules are repelled from the polymer. Adapted from [16]

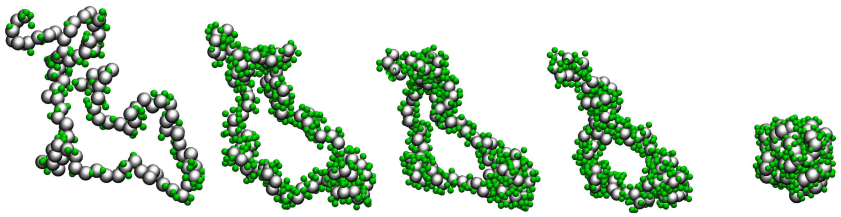

Figure 2.5: Coil to globule transition. The swollen hydrophilic coil state (left) collapses to a hydrophobic shrunken globule state above the LCST (right). Reprinted from [15]

2.3 Chemical Vapor Deposition

Chemical vapor deposition is a technique where a substrate is exposed to one or more gaseous volatile precursors which chemically react in the gas phase and produce a nonvolatile solid on the substrate [5]. CVD can be used to deposit a big variety of materials in crystalline or amorphous form with desired properties.
There exist different types of CVD but there are some basic steps in the CVD process:

1. Transport of the reactants from the gas inlets to the reaction zone.
2. Chemical reaction in the gas phase producing new reactive species.
3. Transport of the reactants and products to the substrate surface.
4. Physical and chemical adsorption.
5. Heterogeneous reactions at the surface leading to film growth.

A schematic drawing of these process steps is shown in fig. 2.6.

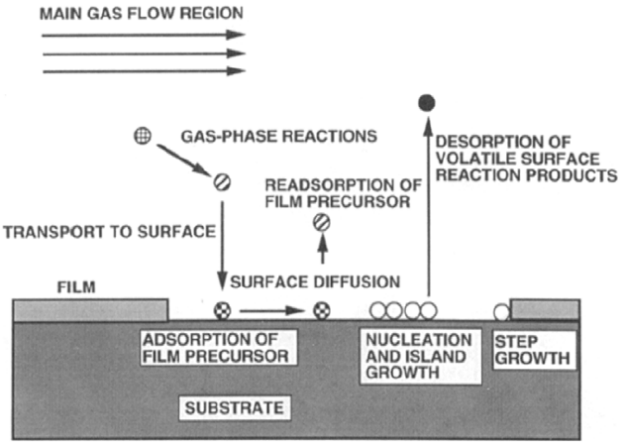

Figure 2.6: Schematic drawing of the main steps in a CVD process. Reprinted from [5]

In CVD polymerization, gas phase monomers are directly converted to thin solid films. When CVD is combined with organic chemistry, it enables depositing polymeric coatings without any solvents which allows the synthesis of monomers that undergo unwanted side reactions in solution and copolymerization of monomers that do not have a common solvent.

2.3.1 Initiated Chemical Vapor Deposition

Initiated chemical vapor deposition is a versatile method for synthesizing polymer thin films. For the iCVD process, a thermal initiator and monomers are introduced into the reactor chamber, where heated filament wires, suspended few centimetres above the surface. The initiator molecules are selectively decomposed by the heated filaments and the resulting fragments react with the monomers adsorbed at the cooled substrate surface and polymerization ensues. An advantage over other CVD techniques is the retention of functional groups which is essential for synthesizing responsive polymers. Furthermore the low substrate temperatures which can be at room temperature allow depositing on thermal sensitive and more complex substrates (e.g. cntact lenses, paper, plastics). [9, chapter 1, p. 8].

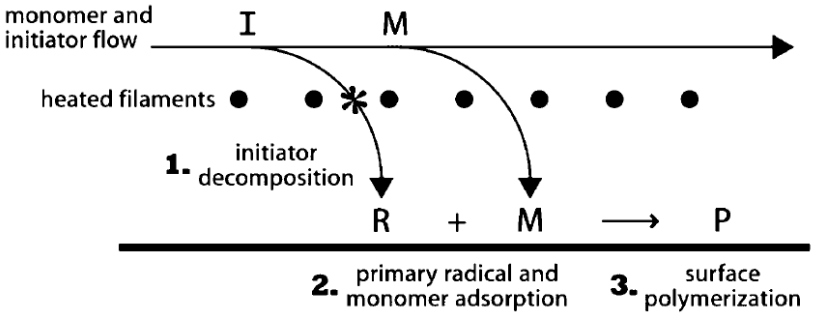

Figure 2.7: Schematic drawing of the iCVD process. Reprinted from [13]

Figure 2.7 shows schematically the major three steps of initiated chemical vapor deposition. In the beginning the reactor chamber is fed with initiator and monomer molecules. Then in the first step the initiator molecules are decomposed at the heated filaments. In the following step, the radicals and the monomer units are adsorbed at the cooled substrate surface, where they react and induce polymerization and film growth in the final step.

2.3.1.1 Conformality

An advantage of using vapor phase deposition techniques for synthesizing polymer coatings is the ability to achieve high conformality on complex substrates because the reactants can diffuse via intermolecular collisions into complex geometries. An example of a conformal polymer film in a trench structure deposited via iCVD is shown in fig. 2.8.
The obtained conformality strongly depends on the so called sticking probability, which is explained in the following section 2.3.1.2.

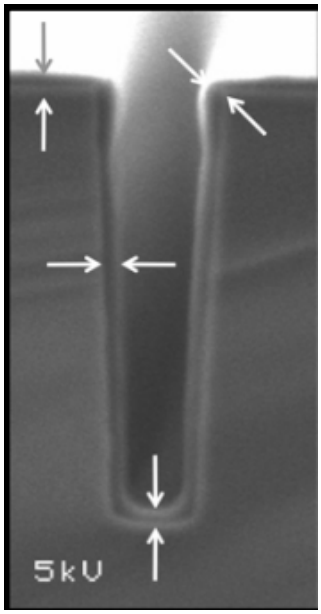

Figure 2.8: Conformal polymer coating in trench structure, obtained by iCVD. Reprinted from [9]

2.3.1.2 Surface reactions and Sticking probability

Polymer CVD has two key steps: transport of reactants from the vapor phase to the substrate and polymerization which occurs mainly at the substrate surface leading to film growth. In general, there are two mechanisms of reactions at the surface, namely the Langmuir-Hinshelwood mechanism where two surface-bond molecules react and the Eley-Rideal mechanism where a molecule from the gas phase collides with a surface bond molecule and is irreversible bonded by chemisorption which is the more likely mechanism in our case due to the fact that the time scale for a surface reaction is one magnitude higher than the surface lifetime of an adsorbed reactant.
An important parameter for the concept of Eley-Rideal surface reactions is the so called "sticking probability", which describes the probability that an impinging gas phase molecule irreversibly sticks to the surface. When the sticking probability is lower than the diffusion rate, conformal deposition is preferred. For the iCVD process, one can imagine the reactive initiator radicals travelling down a trench like it is shown in fig. 2.8 with length L, hitting the wall n times, where it can stick to the wall by chemisorption with the sticking probability Γ. If this probability is high, the film will grow faster at the top of the trench than at the bottom. A method to evaluate this is the step coverage S, which is the of film thickness on top r_t and at the bottom r_b of the trench:

$$S = \frac{r_b}{r_t} = (1 - \Gamma)^n \tag{2.4}$$

For iCVD processes the conformality of a thin film is controlled by the initiator consumption and therefore by the sticking probability of the initiating radicals. The sticking probability increases as the probability of irreversible reaction of the initiating radicals with surface bound monomers increases. Higher monomer surface coverage promotes the sticking probability because the probability for an impinging initiator radical to strike and react to with a monomer is enhanced.
From an practical perspective, the monomer surface coverage can be controlled by changing the working pressure in the reactor, the substrate temperature and the monomer flow rate. [9]

CHAPTER 3

Experimental

3.1 Initiated CVD

3.1.1 Reactor setup

Initiated chemical vapor deposition was used to deposit the polymer films. A schematic drawing of the reactor is shown in fig. 3.1. In the steady state, a medium vacuum with a base pressure around 1 mTorr is present, obtained by a rotary pump (PFEIFFER DUO65). The chemicals, stored in heated chars are led in the chamber via heated lines (100° C), in order to avoid condensation. During the process a fixed working pressure of 250 mTorr was hold constant with help of a butterfly valve for all depositions. The flow rates of the monomers and the initiator were controlled by needle valves. In order to check if the flow rates were set at the desired values, the linear increase of the pressure in the chamber (with disconnected pump) was measured. A chiller (THERMO SCIENTIFIC ACCEL 500LC) was used to hold the bottom of the reactor chamber at a constant temperature. The substrate temperature was varied between 30 and 50° C. As soon as all flow rates were set up to the desired values and the working pressure was reached, the deposition process was started by heating up the filament wires to $200 - 300°$ C.

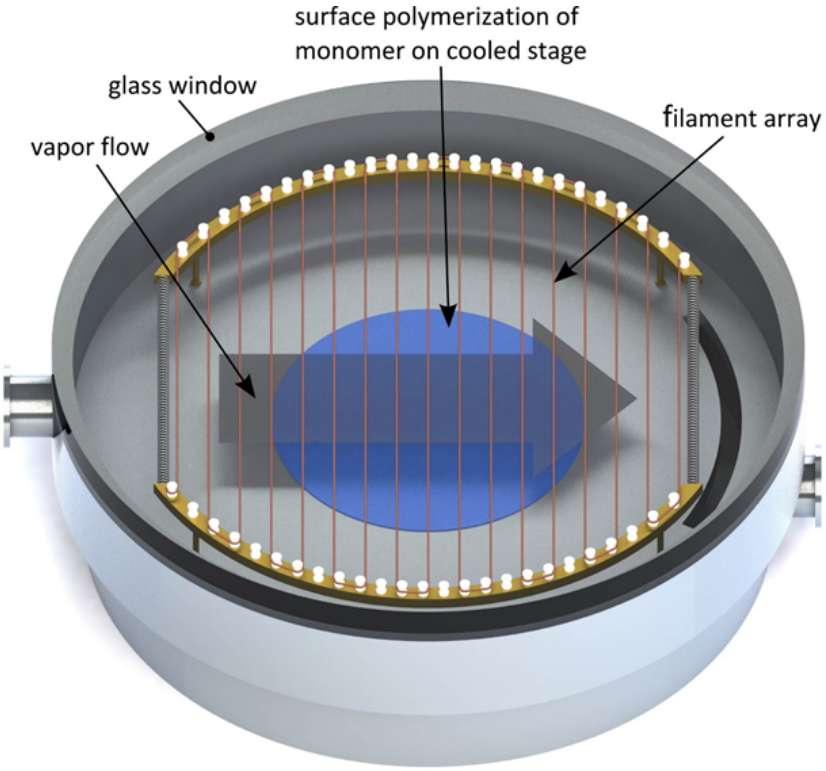

Figure 3.1: Schematic drawing of the iCVD reactor. The reactor is fed with the chemicals through an inlet on the opposite side regarding the pump valves. This leads to a vapor flow through the chamber. The reactor is closed by an glass window. The filament wires are located approximately 2 cm above the substrate stage. The substrate stage can be cooled to enhance surface adsorption.

3.1.2 Monomer Saturation Ratio

The monomer saturation ratio $\frac{P_m}{P_{sat}}$ is an important parameter for CVD polymerization as it determines parameters like the concentration of monomer absorbed on the (substrate) surface, the growth rate or the achieved conformality. It can be calculated from the partial pressure of the monomer P_m and the saturation pressure of the monomer at the substrate temperature of interest, P_{sat}. For a $\frac{P_m}{P_{sat}} = 1$ a liquid will be in equilibrium with the monomer vapor and is undesirable in the iCVD process as it would require physical cleaning of the reactor and long pumping times. Condensation basically occurs on cooled surfaces and can be increased by higher P_m values obtained by a higher flow rate of the monomer. To avoid this, iCVD processes are usually run at $\frac{P_m}{P_{sat}}$ values significantly below 1. In our case we operated with $\frac{P_m}{P_{sat}}$ between 0.1 and 0.7 for the monomers. [9]
The partial pressure of a monomer can be calculated with the following equation 3.1.

$$P_m = \frac{\Phi_m}{\Phi_{tot}} P_{tot} \tag{3.1}$$

where Φ_m and Φ_{tot} describe the flow rate of the monomer and the total flow of chemicals in the reactor chamber respectively and P_{tot} is the total pressure. The saturation pressure can be calculated by using equation

$$P_{sat} = A\ exp\left(\frac{\Delta H_{vap}}{RT_{sub}}\right) \tag{3.2}$$

where ΔH_{vap} is the enthalpy for evaporation, R the gas constant, T_{sub} the substrate temperature and a constant A [6].

3.1.3 Prepared samples

3.1.3.1 p(NIPAAm-co-DEGDVE) depositions

The parameters used for the depositions done in this work are listed in the following tables. Tab. 3.1 shows the flow rates of the chemicals for the prepared p(NIPAAm-co-DEGDVE) thin films.

Table 3.1:
T_sub... Substrate temperature
T_fil... Filament temperature
thickness... Thickness measured by ellipsometry

	Flow rate / sccm					
DEP	NIPAAm	DEGDVE	TBPO	T_sub / °C	T_fil / °C	thickness / nm
1	0,416	0,512	0,912	42	269	224
2	0,409	1,05	0,923	42	270	199
3	0,308	1,08	0,939	50	289	115
4	0,296	0,448	1	47	270	107
5	0,27	0,654	1	38	270	293
6	0,243	1,53	0,506	52	270	117
7	0,381	2,88	1,08	35	270	182
8	0,401	2,2	0,93	35	270	211
10	0,433	1,92	1,14	35	270	140
11	0,506	1,77	1,23	35	270	188
12	0,377	1,29	1,07	40	270	187
13	0,369	0,998	1,19	35	270	324
14	0,352	1,21	1,07	35	230	56
17	0,373	1,01	1,14	33	200	315
18	0,178	0,656	0,428	37	200	55
19	0,171	0,62	0,488	40	300	59
20	0,25	0,714	0,473	35	280	60
21	0,272	0,908	1,02	35	250	0
22	0,218	0,814	0,53	40	260	1042
23	0,27	0,45	0,47	40	290	146
24	0,181	0,511	0,94	32	220	400
25	0,191	0,72	0,72	30	280	360
26	0,283	0,856	0,809	35	216	974
27	0,323	0,89	1,12	35	270	300

Deposition 26 was in 3.1 was deposited on a soft contact lens (type: DAILIES® AquaComfort Plus®). The coated contact lens was used to show

stimuli-induced motion.

In order to obtain a free standing polymer layer deposition 27 in 3.1 was deposited on a sacrificial layer. Therefore a thin polyvinylalcohol layer was first spin coated on a silicon substrate. In details, 19,5 mg PVA were were diluted in 2 ml deionized water and spin coated at 1500 rpm for 60 seconds on several substrates. The thickness of the PVA layer was between 30 and 60 nm, measured with ellipsometry. In a second step, a p(NIPAAm-co-DEGDVE) layer was deposited with the parameters listed for deposition 27 in 3.1 on top.
The PVA layer dissolutes in a water bath and the idea was to fish the swimming polymer thin film with a wire ring.

3.1.3.2 p(DEAAm-co-DEGDVE) depositions

Table 3.2:
T_sub... Substrate temperature
T_fil... Filament temperature
thickness... Thickness measured by ellipsometry

	Flowrate / sccm					
DEP	DEAAm	DEGDVE	TBPO	T_sub / °C	T_fil / °C	thickness / nm
1	0,339	0,867	1,13	35	218	101
2	0,308	0,472	0,956	35	220	102
3	0,564	0,473	0,946	35	220	216

3.2 Chemicals

All chemicals we used were purchased from Sigmar Aldrich and are described in the following section.
The basic material which already bring the functional groups crucial for the termo-responsive properties of the resulting polymers were the two monomers N-Isopropylacrylamide (NIPAAm, fig. 3.2a) and N,N-Diethylacrylamide (DEAAm, fig. 3.2b). The acrylic groups of the monomers in 3.2 are crucial for the hydrophilicity of the material. The additional hydrophilic amide group of NIPAAm enhances the ability to take up water compared to DEAAm. Furthermore due to the slightly more hydrophilic structure of DEAAm, the LCST of this material is supposed to be at higher a temperature [19].
As initiator Di-tert-Butyl peroxide (TBPO, see fig. 3.3a) was used. The labile O-O bond breaks at temperatures higher than 200 $°C$ and forms radicals. At temperatures above 270 $°C$ the radicals undergo a further decomposition, as found by Ozaydin-Ince et. al. in [17].

(a) NIPAAm (b) DEAAm

Figure 3.2: Chemical structure of the functional monomers.

(a) TBPO (b) DEGDVE

Figure 3.3: Chemical structure of the initiator (left) and crosslinker (right).

3.3 In-situ growth control by Laser Interferometry

To have in-situ monitoring of the film growth, Laser-Interferometry was used. A Laser of type (THORLABS HNLS008L-EC) headed through the glass cover on a silicon substrate and the intensity of the reflected beam as a function of time was measured. One wavelength in fig. 3.4 corresponds to approximately 200 nm of polymer film, which can be confirmed by ellipsometry.

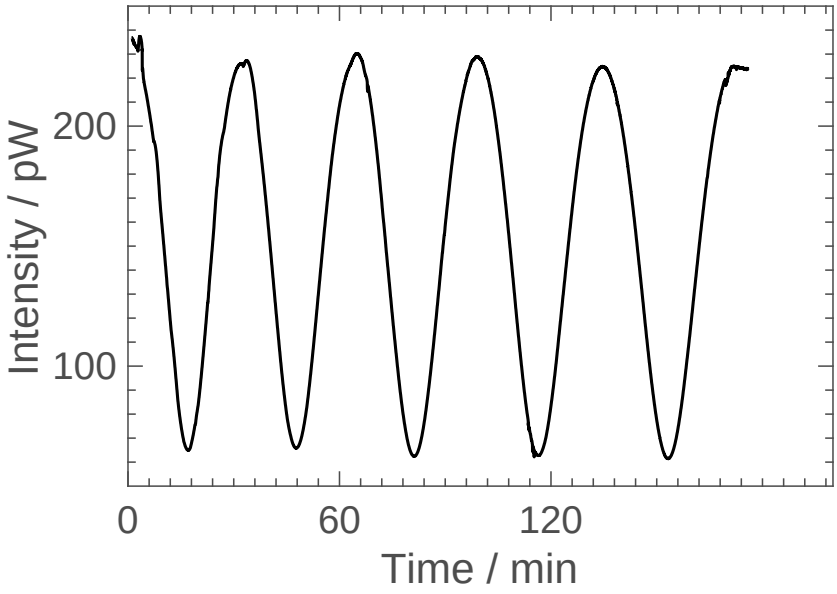

Figure 3.4: In-situ Laser interferometry measurement to monitor film growth. One period corresponds to 200 nm grown film.

3.4 Fourier Transform Infrared Spectroscopy (FTIR)

For chemical analysis of the synthesized films, FTIR measurements were performed. FTIR is a technique to obtain information about the chemical composition of a material by measuring infrared absorption data. The raw data is converted to a spectra by using a Fourier Transform. In our case the used wavelength range was from 400 cm^{-1} to 4000 cm^{-1}. Rotational and vibrational modes of chemical bonds in this wavelength regime are then excited and absorb radiation at a specific wavelength.
The basis of a FTIR sectrometer is a Michelson interferometer as it is shown in fig. 3.5A. A broadband infrared radiation is split by a beam splitter and then travels the two arms to the mirrors, where one has a fixed distance and the other one can be varied. When the two beams recombine at the beam splitter again interference occurs due to path difference of the two beams. The modulated beam then leaves the interferometer, passes through a sample cell and is finally focused on a detector (3.5B). The measured interferogram is then the intensity as a function of the displacement x of the moving mirror from the distance L of the fixed mirror. A computer performs then a mathematical Fourier tranform of the measured data providing a so called single-beam spectrum (3.5C). [10]
The characteristic absorption of the C=O stretch vibrational mode for amides is at wavelength $1640 - 1690\ cm^{-1}$.

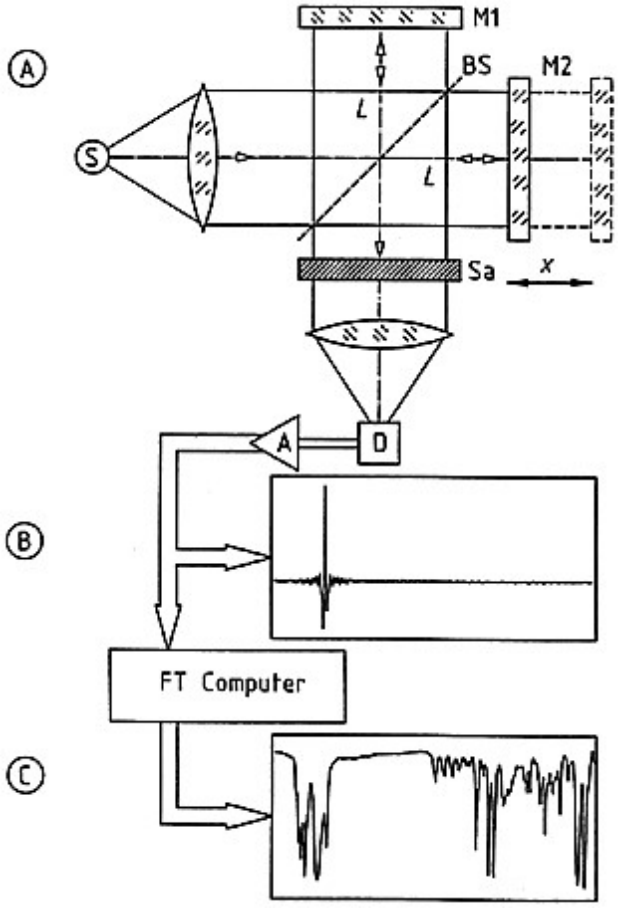

Figure 3.5: Schematic drawing of a FTIR setup.
(A)... Michelson interferometer.
(B)... Sample cell and detector system
(C)... Computer

3.5 Ellipsometry

Ellipsometry uses polarized light to characterize thin film and bulk materials. The light undergoes a change of polarization as it interacts with the sample structure. $tan(\Psi)$ and Δ represent the raw data of an ellipsometry measurement and describe the amplitude ratio of the incident and the reflected light and the phase difference respectively [4]:

$$tan(\Psi)e^{i\Delta} = \frac{\tilde{r_p}}{\tilde{r_s}} \tag{3.3}$$

$\tilde{r_p}$ and $\tilde{r_s}$ in equation 3.3 describe the Fresnel reflection coefficients for the p- and s-polarized light. The obtained data can be modelled for further analysis in order to determine optical constants and film thickness of the investigated materials. For our purpose, also in-situ measurements in liquid water and high relative humidity were performed. For data analysis of measurements performed in laboratory conditions a Cauchy-Model was used:

$$n(\lambda) = A + \frac{B}{\lambda^2} + \frac{C}{\lambda^4} \tag{3.4}$$

The Cauchy model in eq. 3.4 is an empirical relationship between the refractive index n and wavelength λ which allows us to estimate the refractive index by fitting the coefficients A, B and C.

3.5.1 Thickness determination of dry polymer films

For accurate film thickness determination a three angle measurement (65°, 70° and 75°) under laboratory conditions using the "Manual Stage" (see fig. 3.6) were performed.

In fig. 3.7 the recorded data for Ψ and Δ is plotted for the three angles. To analyse the data we used a model with silicon substrate, a 1.7 nm SiO_2 layer on top and a Cauchy layer for our transparent polymer film on the top (see equation 3.4). Figure 3.8 shows a screenshot of the model described. The fitted parameters (optical constants and Cauchy film thickness) are marked in fig. 3.8 with (fit). A screenshot of the model related to the fit in fig 3.7 is shown in fig. 3.8.

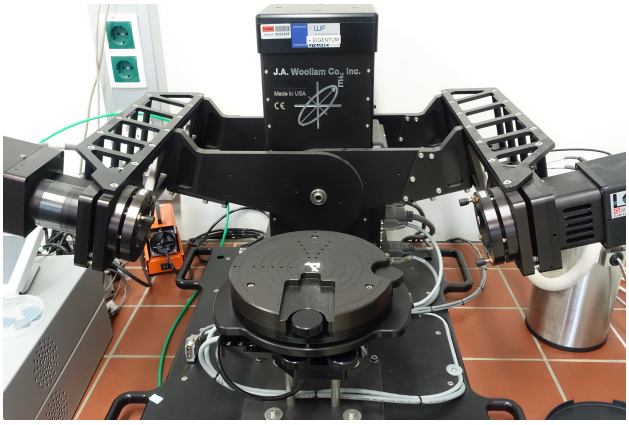

Figure 3.6: Ellipsometer with the Manual Stage mounted. This setup was used in this work for accurate thickness determination of the polymer thin films in dry condition.

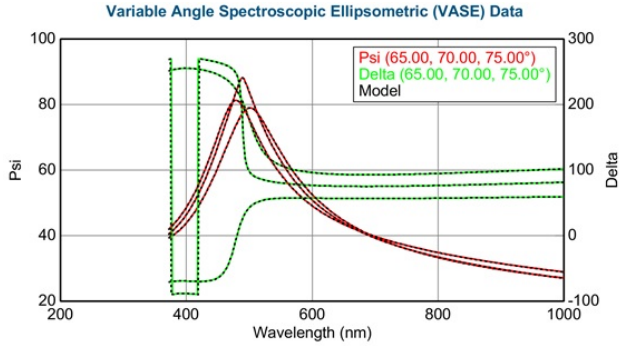

Figure 3.7: Variable angle spectroscopic ellipsometric data for Ψ and Δ for three angles. A Cauchy model was applied in order to fit the data (dotted line). In this representative case, the fitted polymer film thickness was calculated to be (101.08 ± 0.005) nm.

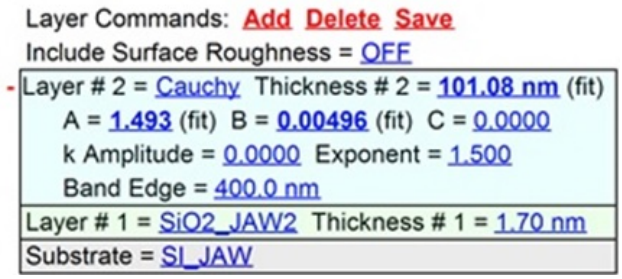

Figure 3.8: Screenshot of the Cauchy model used in CompleteEASE software provided by J.A. Woollam. The optical constants A and B as well as the film thickness of the Cauchy layer were fitted.

3.5.2 In-situ ellipsometry in water

One of the most crucial properties of the synthesized polymer films was the swelling behavior in water, or in other words the increase in thickness due to water uptake when the polymer is exposed to water. In order to get information about swelling we performed in-situ ellipsometry measurements using a different stage. This setup contained a "liquid cell" which could be attached on a flat stage sealed with an o-ring. The cell could be filled with water via a syringe through the tiny holes at the top. For our experiments we used deionized water at room temperature. This setup additionally allowed us to perform experiments at different temperatures or ramping the temperature during the measurement as there was the possibility to heat the sample stage up to 50 $°C$.

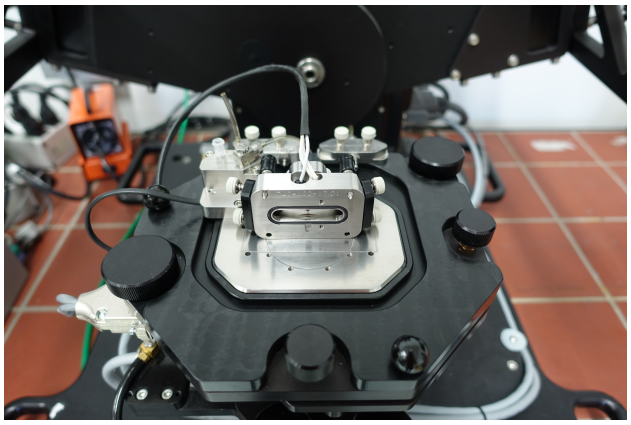

Figure 3.9: Liquid cell setup. The liquid cell was filled with deionized water 30 s after the in-site measurement was started with a syringe. The stage can be heated up to 50 $°C$

Since these measurements were performed in liquid water and the film is expected to take up water, a different modelling approach was used. Effective Medium Approximation (EMA) is used to calculate the optical constants of a mixed material. The calculation is based on mixing optical constants of two constituent materials, the percentage of each material and a depolarization factor. One can imagine the polymer thin film consisting of a matrix of connected polymer chains with voids in between. A schematic drawing is shown in figure 3.10. When the hydrogel is then exposed to water or water vapor, the voids can be filled with water leading to a swollen polymer film.

For our experiments we used a mix of a Cauchy material and water. The software provides three methods of mixing the materials, we used the Bruggemann EMA which assumes spherical inclusions of water in our poly-

mer matrix, when the depolarization factor is set to 0.333. Figure 3.11 shows a screenshot of a used EMA-model.
To get the right optical constants of the Cauchy material, a measurement of the dry film was done right before the in-situ measurements. The optical constants were fitted with the simple model shown in fig. 3.8 and fixed. Then the model was converted to an EMA model, where the thickness and and the percentage of water in the matrix Cauchy material was fitted, as one can see in fig. 3.11.

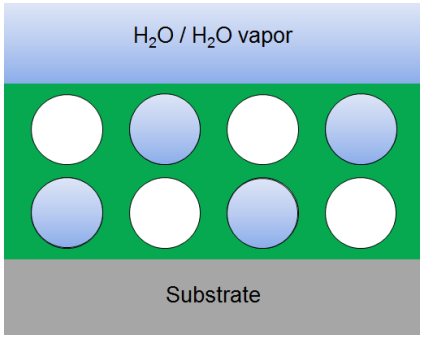

Figure 3.10: Schematic drawing of a swollen polymer film with water in the voids. The polymer matrix is drawn in green with spherical voids (white). When the film is exposed to liquid water or water vapor, the hydrogel can take up water by filling these voids (blue). This behaviour can be modelled with an effective medium approximation (EMA) model.

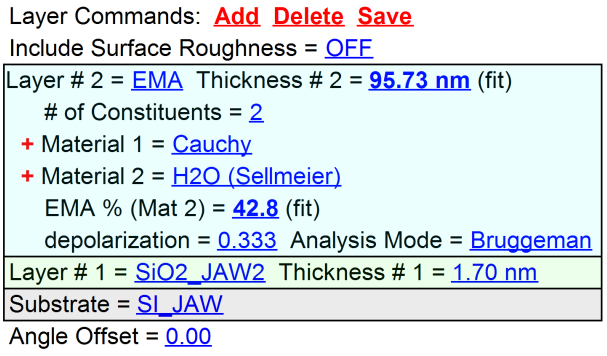

Figure 3.11: Screenshot of a EMA model used in CompleteEASE software provided by J.A. Woollam.

3.5.3 In situ ellipsometry with increased relative humidity at different temperatures.

The setup described in the following was used to perform in-situ experiments in high relative humidity (> 90 % R.H.) while driving temperature ramps in order to investigate the temperature-responsive properties of the thin films. A simple self-built vaporizer made of a small pump and a closed glass container filled with deionized water was used to increase the relative humidity inside the measurement chamber. To monitor the relative humidity during the experiment, a temperature/humidity sensor was placed inside the measurement chamber, next to the sample. Liquid nitrogen allowed us to cool the stage down in this setup, controlled by the temperature control unit (LINKAM LNP95). As the LCST was expected around 32 $°C$ temperature ramps with different heating/cooling rates between 20 $°C$ and 50 $°C$ were performed. An exemplary temperature profile of such an measurement is shown in fig. 3.13.

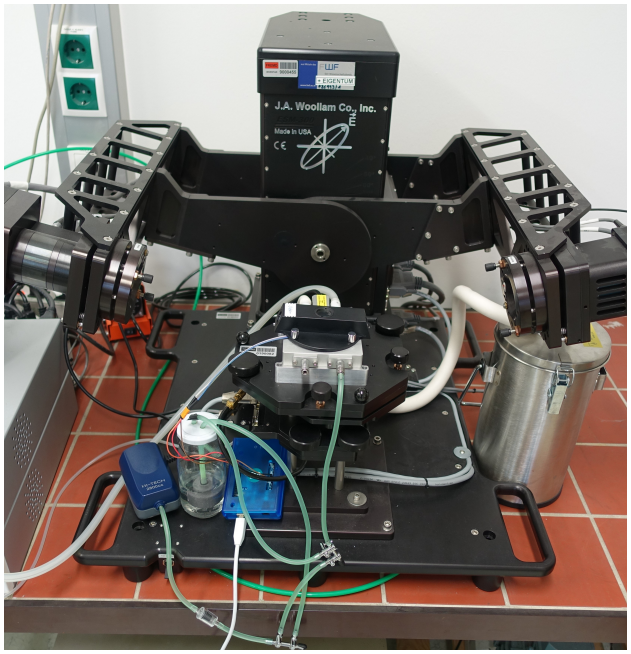

Figure 3.12: Setup for in-situ measurements at enhanced humidity.

For data analysis of measurements in this setup the same model approach as explained in section 3.5.2 was used.

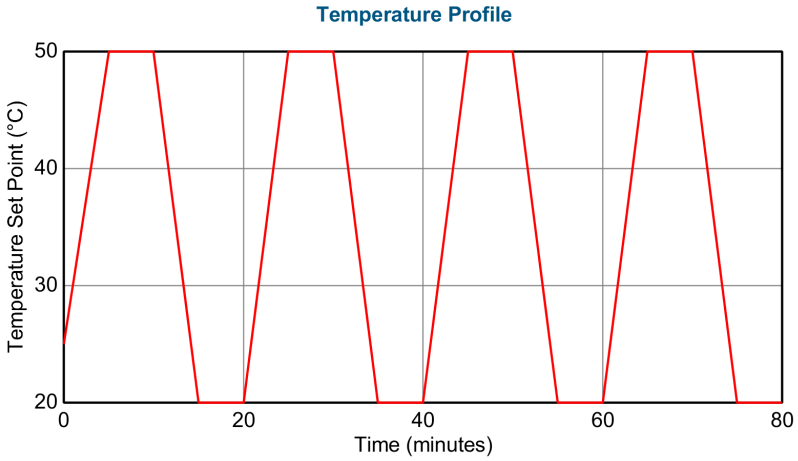

Figure 3.13: Exemplary temperature profile for in-situ measurements at elevated humidity.

3.6 Localized Surface Plasmon Resonance Spectroscopy

Localized surface plasmon resonance spectroscopy uses the existence of plasmons due to interactions of metal subwavelength structures with light. They arise due to the fact that an external electromagnetic field the metal's free electrons are displaced periodically. When the environmental reflactive index changes the polarizability of plasmonic particles changes and thus leads to a shifted surface plasmon resonance. The change of polarizability can be measured by monitoring the scattering spectrum using dark field optical microscopy [14]. A schematic drawing of such an measurement setup can be found in fig. 3.14.

We used SPR spectroscopy to verify the information about the temperature response behavior of p(NIPAAm-co-DEGDVE) films we obtained by spectroscopic ellipsometry.

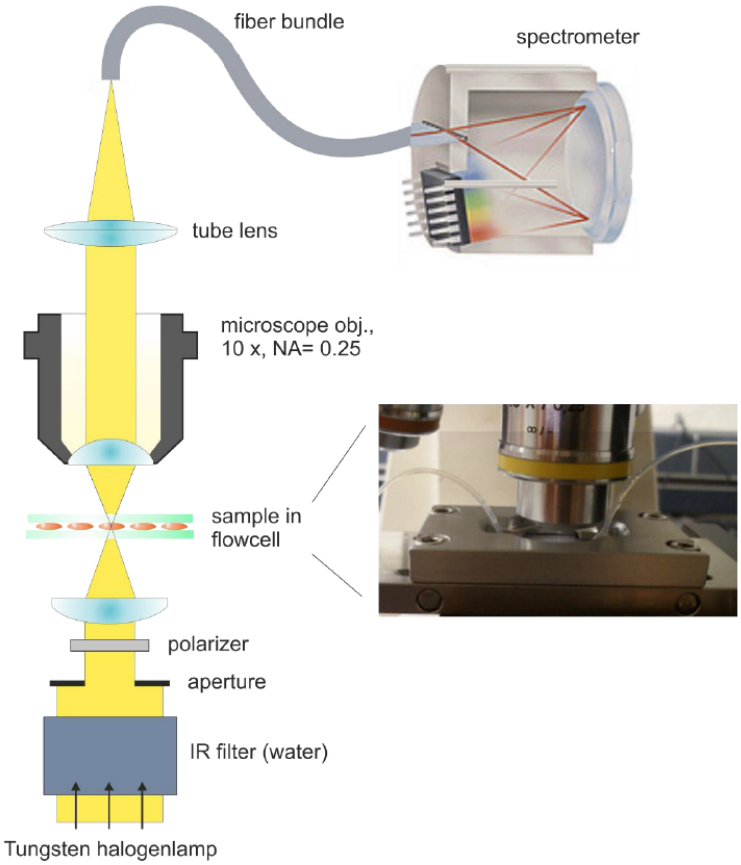

Figure 3.14: Surface Plasmon Resonance spectroscopy setup. Light irradiates the sample, mounted in a flow cell filled with water and entering a optical microscope. The light is then analyzed in a spectrometer. The temperature of the water flowing through the sample flow cell was varied in order to investigate the temperature response of the polymer thin films. Reprinted from [14]

CHAPTER 4

Results

4.1 iCVD process optimization

In order to obtain a fast process with a high deposition rate the substrate temperature was optimized. Several depositions at different substrate temperatures were perfomed and as it was expected, the deposition rate increased for lower substrate temperatures (see fig. 4.1). For temperatures lower than 30 $^{\circ}C$ crystallization at the reactor bottom was observed. To avoid that we found the optimal value for the substrate temperature to be 33 $^{\circ}C$.

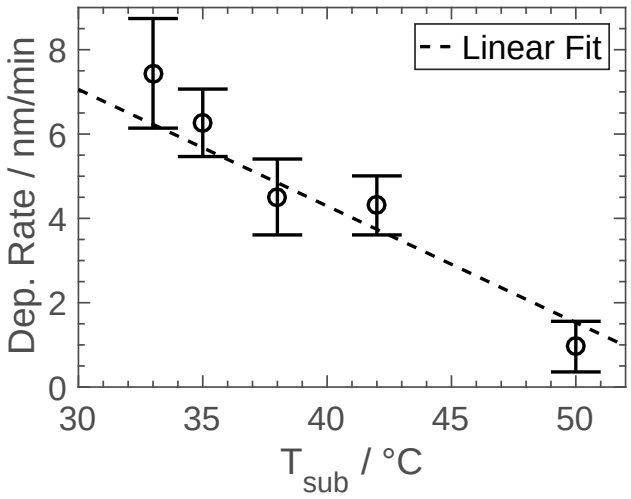

Figure 4.1: Deposition rates for different substrate temperatures. Errorbars calculated from thickness variations of films at different positions in the reactor chamber.

4.2 Parameter tuning for maximum swelling

In the next section parameters which affect the ratio of swelling of the polymer were tuned in order to maximize thickness increase when the thin films are exposed to liquid water (liquid cell, see 3.5.2).
With swelling, the increase of thickness arising due to water uptake is meant and was calculated with equation 4.1.

$$swelling = \frac{t_{fin} - t_{in}}{t_{in}} \tag{4.1}$$

with t_{in} as the initial thickness in the dry state and t_{fin} as the thickness in the swollen state in liquid water. A value of 1 for swelling would mean that the final thickness when the film is swelled in water is double the thickness it was in dry state.

4.2.1 Chemical composition

The ability of taking up water and swelling strongly depends on the ratio of NIPAAm in the synthesized p(NIPAAm-co-DEGDVE) thin films. The more NIPAAm is present in the film the higher is the ability for taking up water at temperatures below the LCST. In this work, samples with several different NIPAAm concentrations were synthesized and tested on their swelling ability. The correlation between the amount of NIPAAm in the polymer and swelling ration is shown in fig. 4.3. At low amounts of the crosslinker DEGDVE below 30% the thin films were not stable anymore and dissolved in water. For that reason we found an optimal DEGDVE ratio of 33% calculated by P_M/P_{sat}. In order to confirm the P_M/P_{sat} calculations, FTIR measurements were performed. A characteristic peak which distinguishes NIPAAm is the $C = O$ amide I peak around 1650 cm^{-1}. Figure 4.2 shows that for decreasing NIPAAm amount the intensity normalized regarding the film thickness decreased. An accurate quantitative chemical analysis was not possible since the co-monomer DEGDVE shows no distinguishable free standing peak in the FTIR spectra.

Table 4.1 lists the initial thickness of the dry polymer films t_{in} and the thickness when swelled in liquid water t_{fin} together with the chemical compositions of the copolymers calculated by P_m/P_{sat}

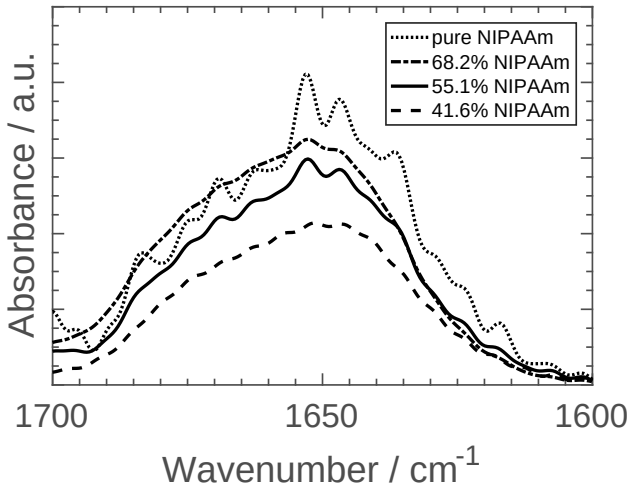

Figure 4.2: Amide I bandpeak for the $C = O$-bond. The intensity was normalized regarding the film thickness and decreased with lower NIPAAm fractions calculated by P_M/P_{sat}.

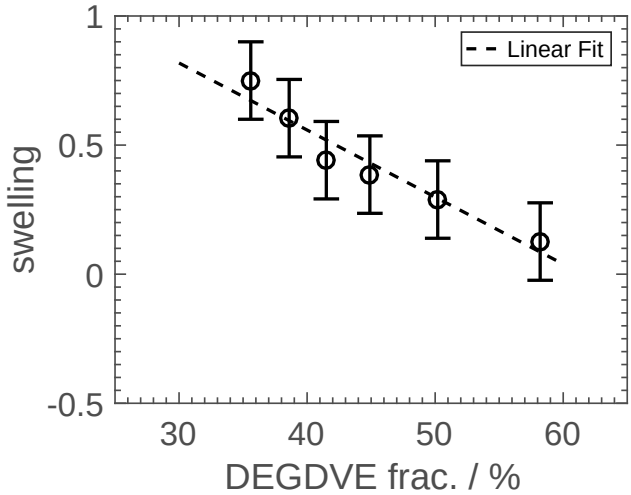

Figure 4.3: The swelling and therefore the ability of taking up water in the polymer network strongly depends on the degree of crosslinking. For increasing amount of the crosslinker DEGDVE the swelling decreased significantly.

Table 4.1: Data corresponding to the depositions represented in fig. 4.3

DEP	t_{in}	t_{fin}	swelling	DEGDVE / %	NIPAAm / %
7	182	205	0,12	58,2	41,8
8	211	272	0,29	50,2	49,8
10	140	194	0,39	44,9	55,1
11	188	271	0,44	41,5	58,5
12	187	300	0,60	38,6	61,4
14	56	98	0,75	35,6	64,4

4.2.1.1 Meshsize

The mesh size of the polymer networks for the different compositions were calculated with the Flory-Rehner theory explained in 2.1.3. The results are listed in table 4.2.

Table 4.2: Calculated mesh sizes for films with different amount of crosslinker

DEP	Mesh size / nm	DEGDVE / %
7	0,98	58,2
8	1,35	50,2
10	1,59	44,9
11	1,73	41,5
12	2,17	38,6
14	2,60	35,6

Figure 4.4 shows that the mesh size decreases with increasing crosslinker amount. This means that the polymer films are denser at high amounts of DEGDVE. This agrees with the swelling behavior of the hydrogels, since the swelling ratio decreases with increasing DEGDVE as it was shown in section 4.2.1 (fig. 4.3). The smaller mesh size decreases the size of the voids in the polymer network and therefore decreases the space for incorporating water in the structure when exposed to water.

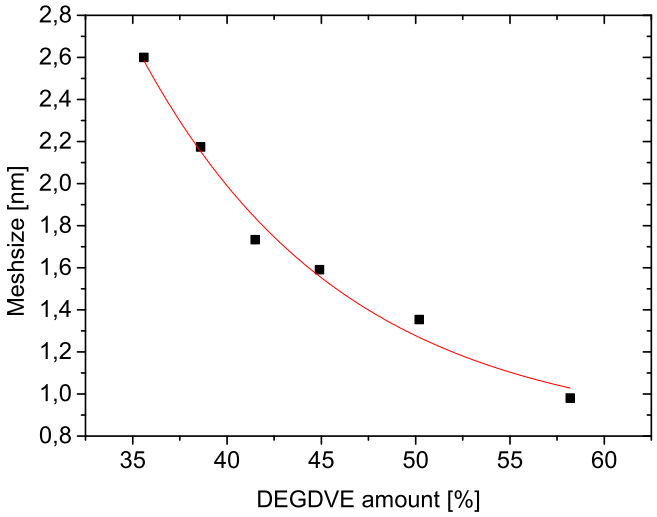

Figure 4.4: The calculated mesh sizes from 4.2 for different amounts of crosslinker DEGDVE. The red line is to help the reader's eye. For increasing DEGDVE the mesh size of the synthesized polymer films decreases.

4.2.2 Filament temperature

The temperature of the heated filament wires during the process influences the ability to swell of the resulting thin films in a way that at higher temperatures not just the amount of initiator molecules but also the species of the radicals change. At temperatures higher than 270 $°C$ an additional decomposition of TBPO takes place as it is reported in [17] (see fig. 4.5). In this high temperature regime, the number of hydrophobic elements incorporated in the polymer network is higher because of the presence of additionally hydrophobic species in the gas phase. A higher amount of methyl and tert-butoxy radicals in the polymer chains lead to an increase in hydrophobicity and therefore decrease the ability to take up water. The relationship between filament temperature and swelling ratio is plotted in fig. 4.6: The swelling ratio decreases with elevated filament temperatures. A drawback of lower filament temperatures is that the deposition rate decreases since the possibility to decompose the initiator molecules to reactive radicals is lower, decelerating the reaction dynamics.

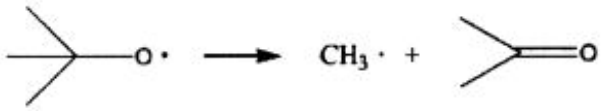

Figure 4.5: At filament temperatures higher than 270 $°C$ an additional decomposition of TBPO radicals takes place. Adapted from [17]

Table 4.3: Data corresponding to the depositions represented in fig. 4.3

DEP	t_{in}	t_{fin}	swelling / $\frac{t_{fin}-t_{in}}{t_{in}}$	DEGDVE / %	T_{fil} / $°C$
11	188	271	0,44	41,5	270
14	42	98	1,23	35,6	230
18	55	97	0,76	41	200
23	146	180	0,23	23,5	290
26	974	1336	0,37	35,7	280

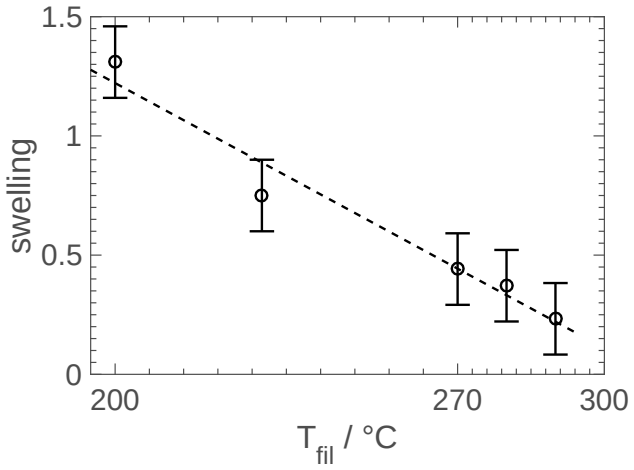

Figure 4.6: At higher filament temperatures the swelling ability of the synthesized films decreased due to more hydrophobic units incorporated in the polymer film.

4.3 Temperature response

The results to the experiments described in 3.5.2 and 3.5.3 are shown in the following section.

4.3.1 Temperature ramps in liquid water

In fig. 4.7 one can see the result of an in-situ ellipsometry experiment where the sample was in liquid water environment over the whole measurement time. One can see that the film thickness of this p(NIPAAm-co-DEGDVE) sample decreases for higher temperatures. The stage temperature was linearly raised from 20 $°C$ to 50 $°C$ in period of 25 minutes. The response to temperature is quite large since the thickness at temperatures $>$ 35 $°C$ is about half the thickness at the initial 20 $°C$. Another noteworthy fact is that the response the change in thickness mainly happens at temperatures between 20 $°C$ and 35 $°C$ which is more cleary to see in fig. 4.8. In this hydrophilic state not all water is repelled since the thickness arrives around 65 nm at high temperatures in fig. 4.8 whereas a thickness in a dry state measured in air a thickness of 59 nm was found. The transition seems not to happen at a specific temperature, but more in a more broad range. This can be explained by assuming that the polydispersity in our film is quite high, which means that we have different structured polymer chains present in our sample, which exhibit the coil to globule transition at different temperatures.

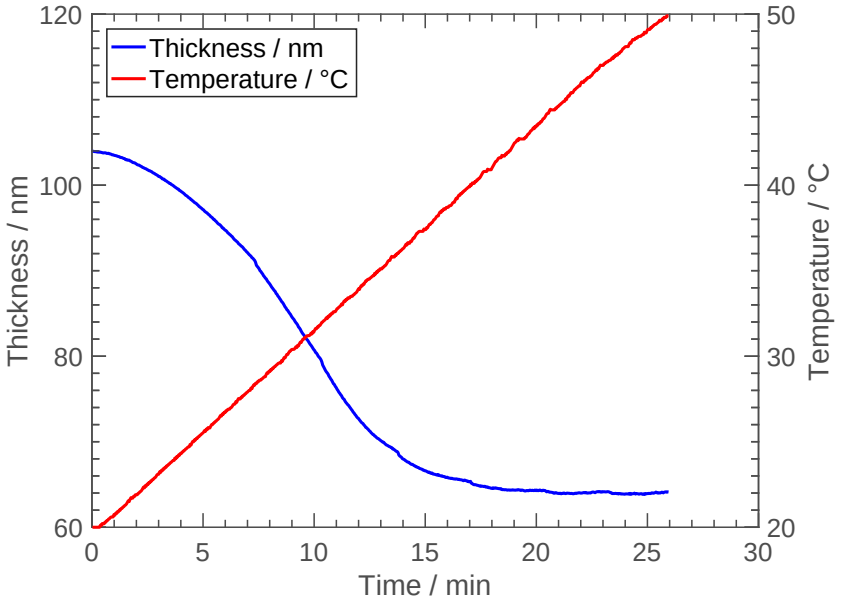

Figure 4.7: In-situ ellipsometry measurement in liquid water. The temperature of the sample stage was heated linearly from 20 $°C$ to 50 $°C$ in a period of 25 minutes. The p(NIPAAm-co-DEGDVE) film collapsed to almost half of the initial thickness when the temperature exceeded it's LCST.

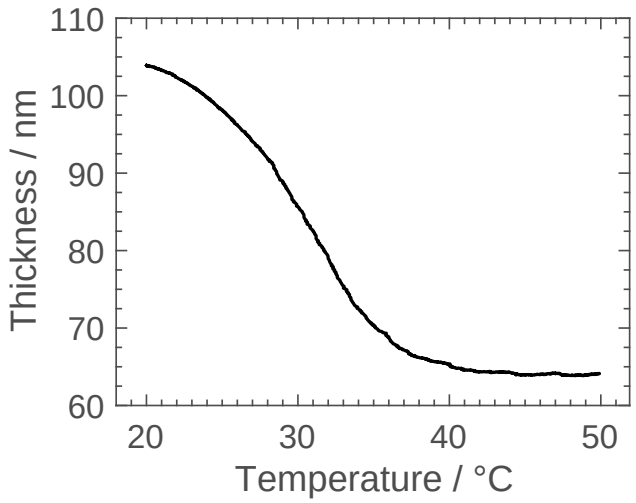

Figure 4.8: Temperature dependency of the film thickness obtained by an in-situ ellipsometry measurement in liquid water. The film thickness decreases with increasing temperature. The thickness changes over a broad temperature range between 20 $°C$ and 35 $°C$.

4.3.2 Temperature ramps in humid air

With the setup described in section 3.5.3 we had the possibility to cool the sample stage. This gave us the opportunity to investigate how the sample behaves when approaching the transition from the other side, starting at high temperatures where the polymer is in the hydrophobic shrunken state.
In order to obtain information about the reversibility and reproducibility the temperature was cycled several times during one measurement. The results for a p(NIPAAm-co-DEGDVE) sample are shown in the following. In fig. 4.9 one can see that the film thickness follows the temperature profile. When the sample is heated, the film undergoes a LCST transition to a hydrophobic shrunken state where the polymer collapses and the thickness rapidly decreases to a value close to the thickness we measured in a dry environment (dry state: 56 nm). When the stage was cooled back to 20 $°C$, the film thickness jumps up to the initial value around 100 nm, since we are at a temperature below the LCST where the polymer is in a hydrophilic state and takes up water from the vapor phase.

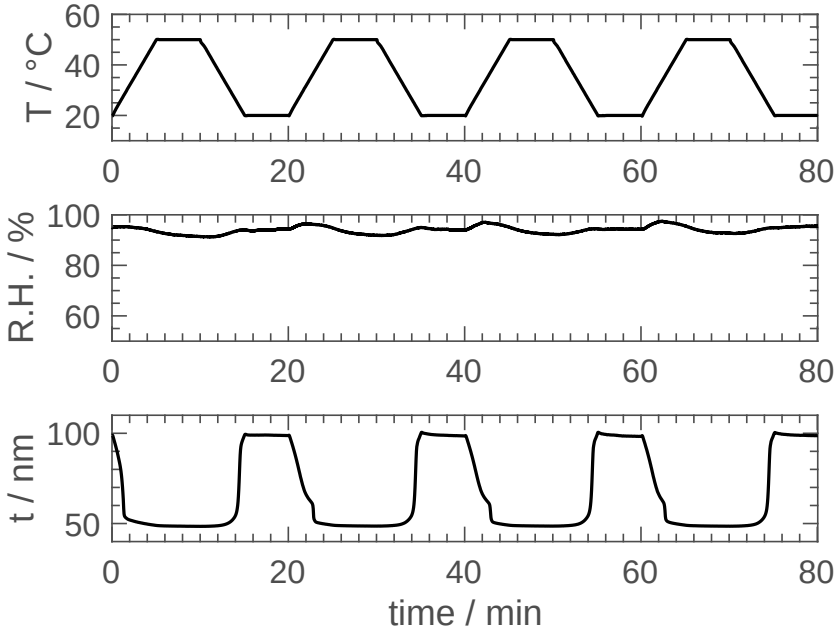

Figure 4.9: Upper plot: Temperature profile: Four cycles of heating from 20 $°C$ to 50 $°C$ in 5 min, holding the temperature for 5 min, then cooling back to 20 $°C$ and holding for 5 min again.
Middle: The relative humidity in the measurement chamber was hold constant above 90% over the whole measurement.
Lower plot: Fit result for the film thickness obtained by an EMA model.

Figure 4.10 shows the temperature dependency of the film thickness for the four cycles. To interpret this plot one has to follow the graph clockwise by starting at high thickness and low temperature and then going on the upper way to lower temperatures during heating before going the lower path back to high thickness when arriving at low temperatures. A difference for the heating and cooling cycle is clearly noticeable. First, the temperature at which the transition seems to take place strongly differs for heating and cooling respectively. For the cooling process the temperature at high response lies more than 10 $°C$ lower compared to the heating. Secondly, the first cycle (red) has a different, more sharp shape concerning the heating path than the following cycles. This particular behaviour is not fully understood so far. Andersson et al. found in [2], where they described the swelling process of NIPAAm films with the diffusion equation, a difference in heating and cooling processes. The shrinking process, when the temperature is increased to a temperature above the critical temperature could not be fitted with the model they used. They suggest that the difference arises from the change in the friction between polymer network and solvent due to the large decrease of hydrogen bonds between water molecules and polymer network. For thicker films, problems associated with a compact skin at the surface of the polymer film are suggested by Tanaka et al. in [20] where they found the shrinking process to have three different time domains with a first shrinking period followed by a plateau period and a second shrinking process. This three time domains are similar to what can be seen in figure 4.10. Tanaka et al. explained the three time domains qualitatively as follows: In the first period, the swollen hydrogel shrinks in a thin surface region only. This collapsed dense polymer network layer is then impermeable for the inner fluid and prevents further shrinking resulting in the second plateau period. The inhomogeneity of density and osmotic pressure relax during the plateau period. The surface layer is then not impermeable anymore and the film starts to shrink again. The heating paths for the cycles 2, 3 and 4 with the bend around 37 $°C$ furthermore indicate that the shrinking process happens not in an equilibrium state. The path of the first temperature cycle, when the film was not exposed to high humidity before differs from the following cycles. This may occur from the polymer network rearranging when taking up water the first time.

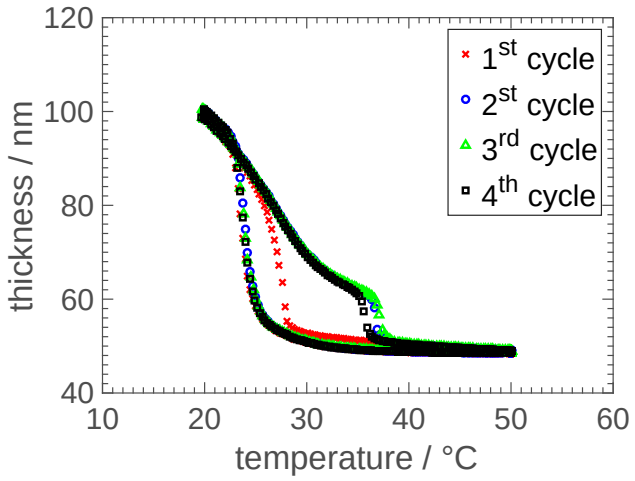

Figure 4.10: The temperature dependence of the film thickness of a p(NIPAAm-co-DEGDVE) sample for four cycles of stage temperature variation. The thickness decreases when the stage was heated up (upper path) and jumped back to the initial thickness when the stage was cooled down to 20 $°C$ (lower path). There is a clear difference in the heating/cooling process visible. Furthermore the heating path of the first cycle differs from the other cycles.

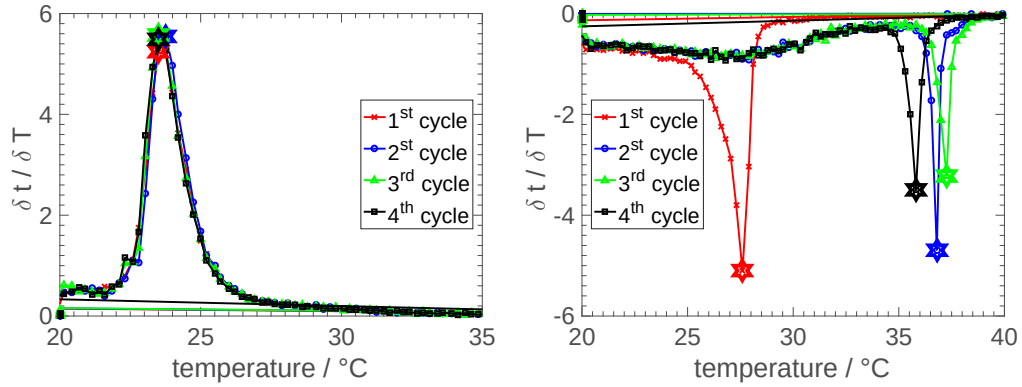

(a) cooling (b) heating

Figure 4.11: First derivative of the data shown in fig. 4.10 for cooling and heating respectively. In 4.11a one can see that the temperature at which the change in thickness and therefore the response is maximum is the same for all cycles during cooling, whereas for heating in fig. 4.11b it is different. The response temperatures differs for the first cycle from the following.

The first derivative of the data in fig. 4.10 emphasizes the the temperatures where the change in thickness is at a maximum. The following two plots show these temperatures for cooling and heating respectively. In plot 4.11a the response when the sample was cooled is at the same temperatures for all 4 cycles around 23 $°C$ wheras for heating plot 4.11b shows a big gap for the transition temperature between the first cycle (28 $°C$) and the following three cylces (36 $°C$).

4.3.3 poly(DEAAm-co-DEGDVE)

In order to obtain hydrogels with a different LCST, we used N,N-Diethylacrylamide (DEAAm) instead of NIPAAm crosslinked with DEGDVE. The chemical structure of the monomers were shown in section 3.2 (fig. 3.2). Using DEAAm, we expected two differences regarding the swelling behaviour of the polymer thin films. First, due to the absence of a hydrophobic CH group, a higher LCST compared to the prepared p(NIPAAm-co-DEGDVE) samples is expected, like it was shown in literature by Pena-Francesch et al. in [19]. Besides a change of the LCST we also expected the swelling ratio to decrease due to the lack of NH moieties to form intermolecular hydrogen bonds to take up water.

4.3.3.1 Chemical composition

The chemical composition of the prepared p(DEAAm-co-DEGDVE) polymer thin films was analysed by FTIR. Again the characteristic peak of the responsive DEAAm is the C=O amide I peak around 1650 cm^{-1}. The full spectrum of a p(DEAAm-co-DEGDVE) copolymer is shown in fig. 4.12a. In fig. 4.12b one can see that the intensity of the C=O peak which is characteristic for DEAAm decreases as the amount of DEGDVE is increased. This agrees with the values calculated form P_m/P_{sat}.

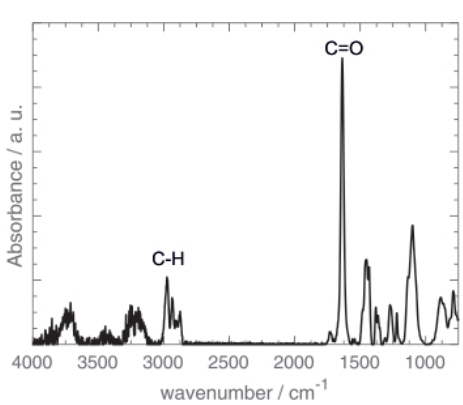

(a) full FTIR spectra of p(DEAAm-co-DEGDVE)

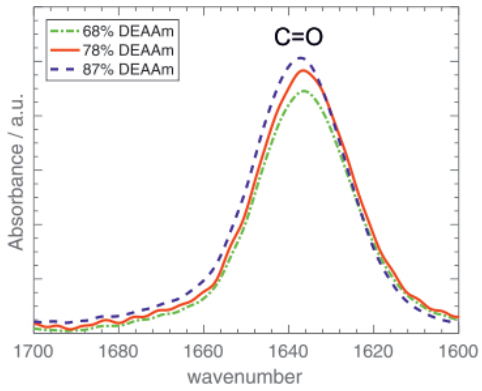

(b) Characteristic C=O peak of DEAAm decreases with higher amount of the crosslinker DEGDVE

Figure 4.12: Intensity of C=O amide I peak decreases for higher DEGDVE ratios. This validates the values calculated by P_m/P_{sat} qualitatively.

In this work samples with three different ratios of DEAAm and DEGDVE were prepared and all were found to be stable. In order to find the optimum

composition to obtain maximum swelling and durable films as it was done for the p(NIPAAm-co-DEGDVE) samples (section 4.2.1) further deposition with decreasing DEGDVE need to be done.

4.3.4 Temperature ramps in liquid water

The p(DEAAm-co-DEGDEVE) films were investigated on their temperature responsive behavior with the same measurements as in 4.3 for the NIPAAm copolymers. At first, a temperature ramp in liquid water (setup see 3.5.2 measurement was performed. The polymer film decreased in thickness as expected for higher temperatures, with the difference to p(NIPAAm-co-DEGDVE) films (fig. 4.7) that the thickness further decreased linearly at temperatures higher than 35 $°C$, which is shown in fig. 4.7. This is an indication for an elevated LCST since the transition to a hydrophobic water repelling state seems not fully executed. The setup is limited to a maximum temperature of 50 $°C$, therefore we could not find the temperature range where the thickness reaches it's lower limit. The change of thickness due to dehydration above the LCST is lower for DEAAm compared to NIPAAm (fig. 4.7) which can be explained by looking at the chemical structure differences of DEAAm and NIPAAm. Due to the lack of NH moieties in DEAAm it is not possible to form intramolecular hydrogen bonds like NIPAAm does in the dehydrated state [19].

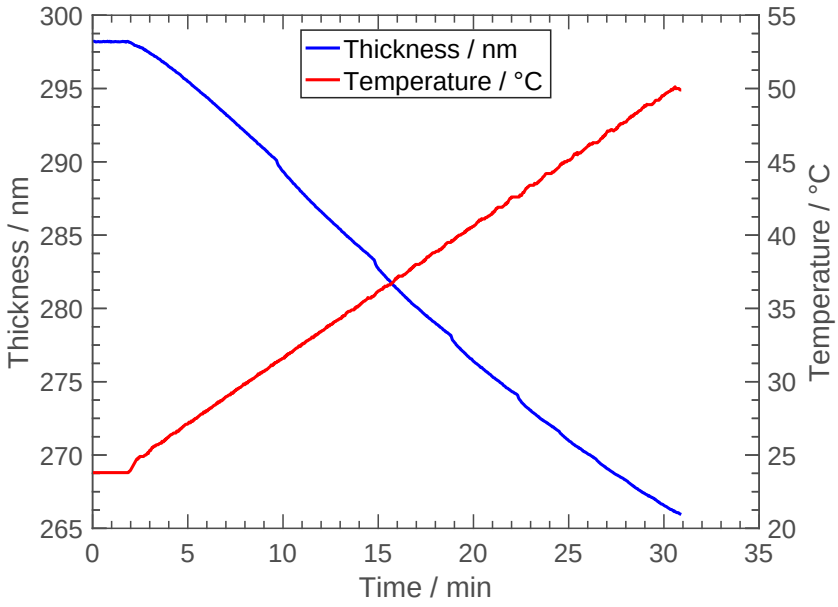

Figure 4.13: In-situ ellipsometry measurement in liquid water of a p(DEAAm-co-DEGDVE) sample while ramping the temperature from 25 $°C$ to 50 $°C$. The thickness of the polymer film decreased linearly over the whole temperature range.

4.3.5 Temperature ramps in humid air

Simultaneously to the experiments described in section 4.3.2 in-situ ellipsometry measurements in humid air environment and cycled stage temperature were performed to investigate the temperature responsive behavior of the prepared p(DEAAm-co-DEGDVE) films. The results are shown in fig. 4.14. The data shown in fig. 4.14 shows similar behavior to the measurements on p(NIPAAm-co-DEGDVE) samples (see fig. 4.9). The polymer film collapses when the temperature is raised and jumps back to the initial value when the stage is cooled back to 20 $°C$. Again the relative humidity inside the measurement chamber was constant above 90 %.
For further analysis the thickness was plotted as function of temperature (fig. 4.15). Equal to fig. 4.10 one has to follow the graph clockwise, starting at high thickness and low temperatures, following the upper path where the sample was heated and going back the lower path back to the initial thickness. The temperature where the transition takes place is different for heating and cooling processes, which is emphasized in fig. 4.16, where the first derivative of fig. 4.15 is plotted. In this plot one can see that the temperature for which the change in thickness and therefore the response is the maximum is firstly different when the sample is heated or cooled. It seems like the response is delayed, since the response temperature is higher when coming from low temperatures than when the sample is cooled. This hysteresis is not reported in literature so far.

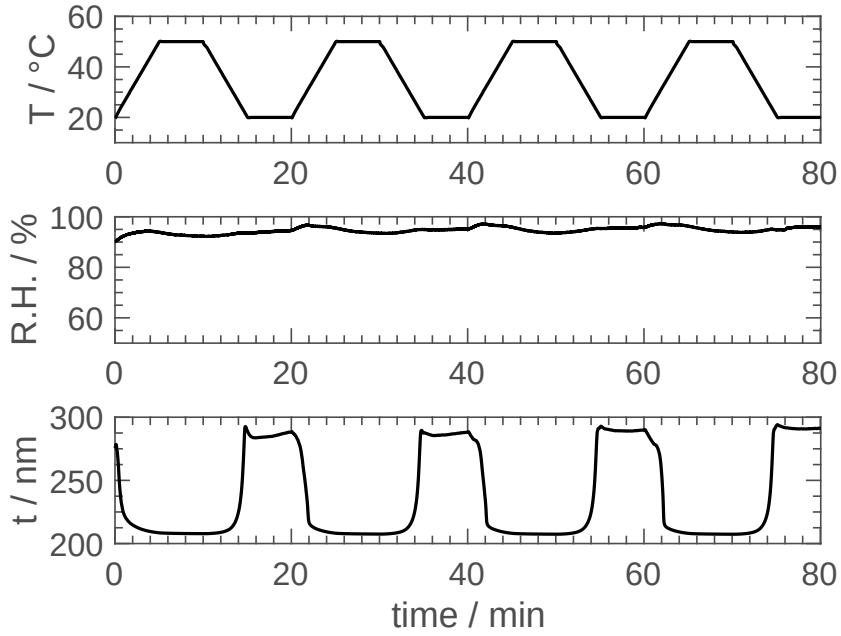

Figure 4.14: Upper plot: Temperature profile: Four cycles of heating from 20 $°C$ to 50 $°C$ in 5 min, holding the temperature for 5 min, then cooling back to 20 $°C$ and holding for 5 min again.
Middle: The relative humidity in the measurement chamber was hold constant above 90% over the whole measurement.
Lower plot: Fit result for the film thickness obtained by an EMA model.

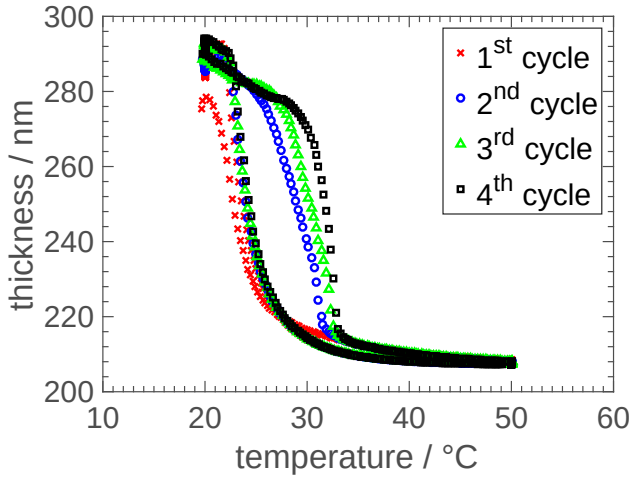

Figure 4.15: The temperature dependence of the film thickness of a p(DEAAm-co-DEGDVE) sample for four cycles of stage temperature variation. The thickness decreases when the stage was heated up (upper path) and jumped back to the initial thickness when the stage was cooled down to 20 $°C$ (lower path). There is a clear difference in the heating/cooling process visible. Furthermore the heating path of the first cycle differs from the other cycles. This behavior is similar to the one observed for the p(NIPAAm-co-DEGDVE) sample.

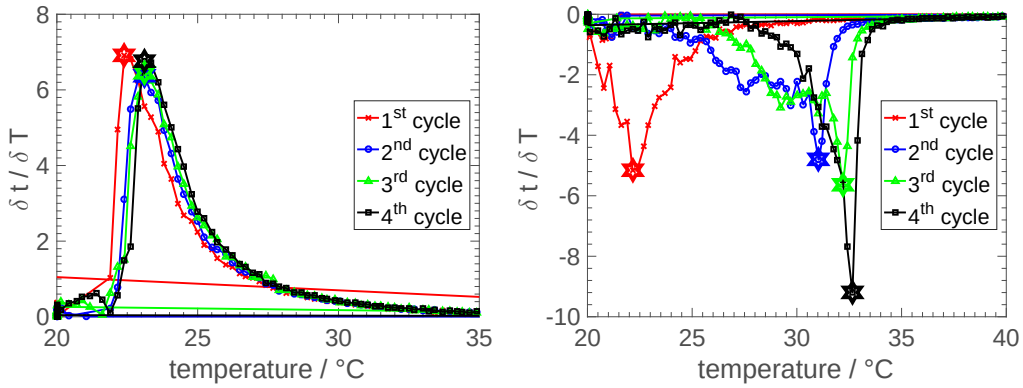

(a) cooling (b) heating

Figure 4.16: First derivative of the data shown in fig. 4.15 for cooling and heating respectively. In 4.16a one can see that the temperature at which the change in thickness and therefore the response is maximum is the same for all cycles during cooling, whereas for heating in fig. 4.16b it is different. The response temperatures differs for the first cycle from the following equally as it was found for p(NIPAAm-co-DEGDVE) in fig. 4.11

4.4 Surface Plasmon Resonance Spectroscopy

SPR measurements were done to get further information about the LCST of our prepared p(NIPAAm-co-DEGDVE) polymer thin films. The results have to be seen with caution, since the measurement setup was not ideal for our purpose, since there was a large difference in heating and cooling rates, which means that the polymer was not in equilibrium during the measurements. Furthermore just two samples could be measured with SPR which makes it difficult to make a clear statement on the quality of the measured data.
Figure 4.17 shows the shift of the resonance position (blue) over time and the temperature profile (red) applied to the sample. From the plotted temperature one can clearly see the difference timescales of heating and cooling processes. The resonance position seems to follow the temperature profile, as the slope is higher during the faster heating process.
On the other hand, fig. 4.18 where the resonance position is plotted versus the temperature, we observe something similar to what we have seen in section 4.3.2 where we did in-situ ellipsometry measurements in humid air while cycling the temperature (fig. 4.10). While the drift of the resonance position during heating is maximum between 20 $°C$ and 35 $°C$ it seems that for cooling the polymer film responds during cooling at temperatures below 20 $°C$. Temperatures below 15 $°C$ were not accessible due to fogging windows.

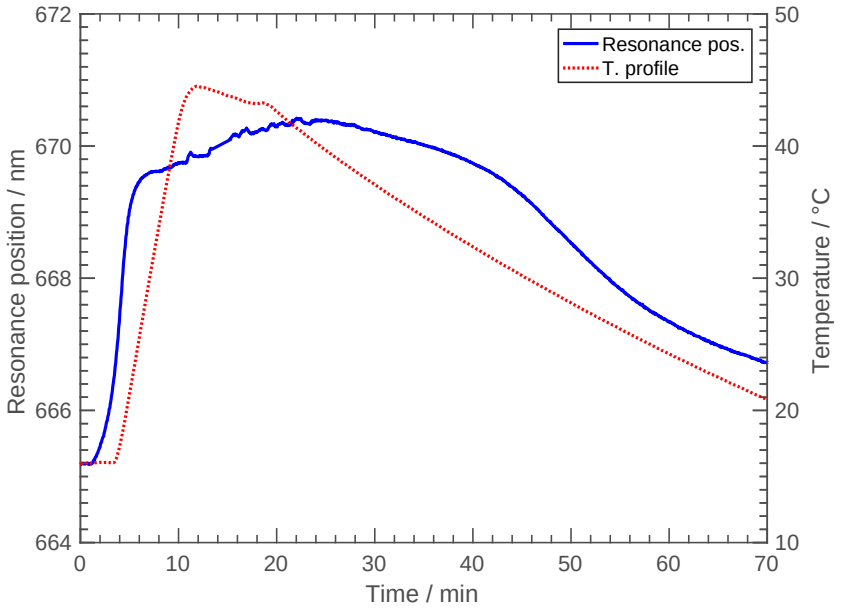

Figure 4.17: Temperature profile and surface plasmon resonance position for a sample of the p(NIPAAm-co-DEGDVE) series. The resonance frequency follows the temperature profile.

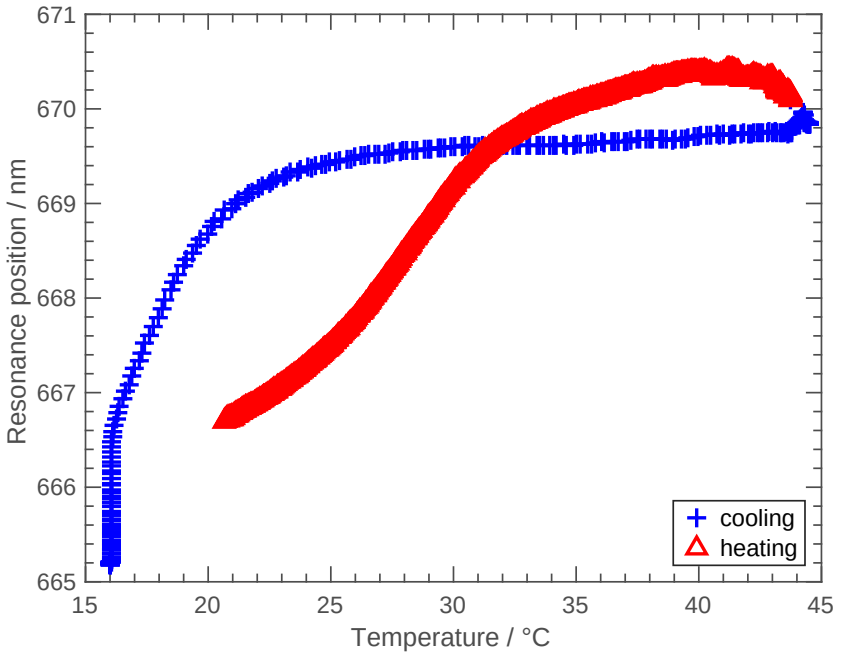

Figure 4.18: Surface plasmon resonance position dependence of temperature for p(NIPAAm-co-DEGDVE).

4.5 Stimuli-induced Locomotion

During this work different attempts to design some kind of movable device were made. As substrates we used among others simple printing paper, Kapton-strips, plastic foils, Polydimethylsiloxane or even contact lenses. Fig. 4.19 shows a deposition on paper with silver ink lines. The idea was to heat the silver lines by applying a voltage and obtain this way a bending of the paper in humid air conditions. Unfortunately we could not detect any movement due to the temperature response of the deposited polymer. A reason could be that the synthesized polymer layers in the sub-micrometer range were too thin to bend a rigid substrate like paper by swelling and shrinking. More successful experiments are described in the following.

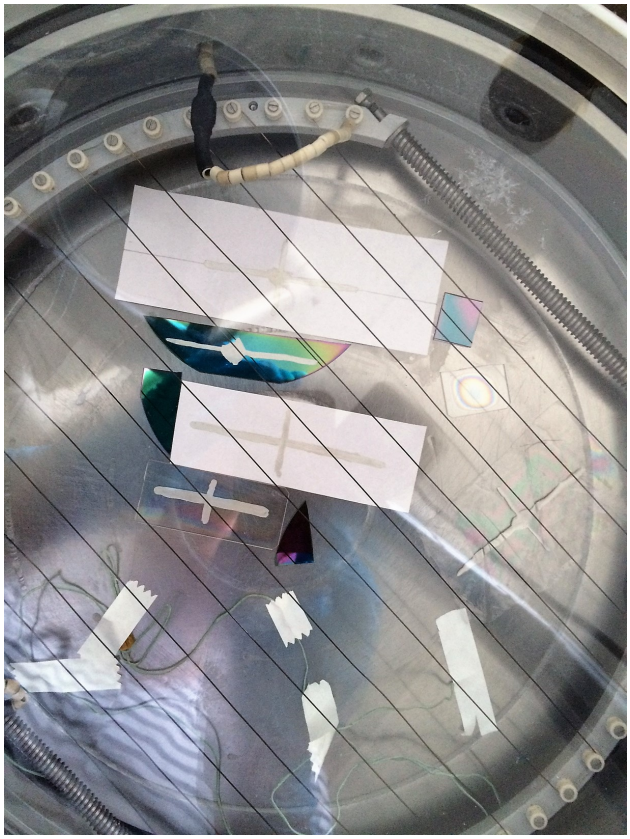

Figure 4.19: Paper with silver ink lines was used as substrate. The idea was to heat the silver paint and in this way apply a temperature gradient to the polymer deposited on top.

4.5.1 Stimuli-responsive depositions on contact lenses

The low temperatures in a iCVD allowed us to deposit p(NIPAAm-co-DEGDVE) films on thermo-sensitive substrates, like contact lenses. The thickness of the thin film deposited on the contact lens could not be measured directly, but a reference sample on a silicon wafer gave 1000 nm polymer film measured by ellipsometry. In order to see some movement, we set up a experiment where the contact lens was immersed in a water bath. When the contact lens arrived at the glass bottom the water was heated up from room temperature with a heating plate to approx. 60 $°C$. The whole experiment was filmed with a smartphone. At some point in the experiment, the contact lens started to bend first and then shrunk and forming wrinkles at higher temperatures. Two screenshots of the recorded video clip are below.

(a) Swollen state. (b) Shrunken state.

Figure 4.20: Experiment with a contact lens coated with a p(NIPAAm-co-DEGDVE) film.

4.5.2 Free standing films

Free standing p(NIPAAm-co-DEGDVE) polymer films with the method of using a sacrificial layer as it is described in 3.1.3. We were able to fish a polymer thin film with a metal ring from a water bath which can be seen in fig. 4.21. A photo of the free standing polymer thin film right after taking it out of the water bath is shown in fig. 4.21a. The hydrated free standing film was then placed on a heating plate which was set to a temperature of 80 $°C$. After some time, when the temperature exceeded the LCST, the polymer film collapsed and expelled the water, as one can see in fig. 4.21b. We were able to reproduce the swollen free standing film by immersing the collapsed film back into the water bath and fishing it again with the wire ring.

(a) Swollen state.

(b) Shrunken state.

(c) Re-hydrated free standing film

Figure 4.21: Experiment with a free standing p(NIPAAm-co-DEGDVE) film. The hydrated thin film fished with a wire ring from the water was placed above a heating plate. When the temperature exceeded the hydrogel's LCST, it repelled the water and collapsed. It was possible to re-hydrated the collapsed film again by immersing it in a water bath again.

CHAPTER 5

Conclusion and Outlook

Stable thermo-responsive polymer thin films could be synthesized with initiated chemical vapor deposition and were investigated on their response to humidity and temperature. Copolymers of NIPAAm and DEGDVE were stable above a DEGDVE fraction of 33 %. All synthesized copolymers of DEAAm and DEGDVE were found to be stable, where the lowest used DEGDVE fraction was 13 %. In order to get a high deposition rate and a stable process, a substrate temperature T_{sub} of 35 $°C$ was found to be optimum.
In order to maximize the swelling of p(NIPAAm-co-DEGDVE) films, a filament temperature T_{fil} was found to be ideal at 200 $°C$. Maximum swelling was found to be 2.33, in order words the thickness of a the polymer coating more than doubled when exposed to liquid water.
The response to changes in temperature was studied for both p(NIPAAm-co-DEGDVE) and p(DEAAm-co-DEGDVE) films. For both the transition from a hydrated hydrophilic state below their LCST to a shrunken hydrophobic state at high temperatures could be observed. The response was higher for p(NIPAAm-co-DEGDVE). On the other hand, the response temperature range could be extended to higher temperatures (linear response between 20 $°C$ and 50 $°C$) when co-polymerizing DEAAm and DEGDVE.
The results on the in-situ ellipsometry measurements we performed under high relative humidity and cycling stage temperature conditions are not fully understood yet and should be investigated further. It was found for both, p(NIPAAm-co-DEGDVE) and p(DEAAm-co-DEGDVE), that the transition from hydrophilic to hydrophobic is different as the the other way around (see fig. 4.10 and 4.15. This phenomenon is not fully understood in literature.

The response to temperature changes in terms of change in thickness observed in these experiments were remarkable, as the thickness in fig. 4.9 was around 50 nm at high temperatures and jumped up to almost 100 nm a low temperatures.
Regarding attempts to achieve macroscopic movements triggered by thermoresponsive polymers it could be shown that a contact lens coated with a 300 nm p(NIPAAm-co-DEGDVE) copolymer film bent in liquid water when the heated. In order to apply a temperature gradient by creating some kind of actuator array, a suitable substrate needs to be found.

List of Figures

List of Tables

Bibliography

[1] Mahriah E Alf, Paul D Godfrin, T Alan Hatton, and Karen K Gleason. Sharp hydrophilicity switching and conformality on nanostructured surfaces prepared via initiated chemical vapor deposition (icvd) of a novel thermally responsive copolymer. *Macromolecular rapid communications*, 31(24):2166–2172, 2010.

[2] Matz Andersson, Anders Axelsson, and Guido Zacchi. Swelling kinetics of poly (n-isopropylacrylamide) gel. *Journal of controlled release*, 50(1):273–281, 1998.

[3] Peter William Atkins and Julio De Paula. *The elements of physical chemistry*, volume 3. Oxford University Press New York, NY, USA:, 2005.

[4] J.A. Woollam Co. Ellipsometry faq. `https://www.jawoollam.com/resources/ellipsometry-faq`. Accessed: 31.03.2017.

[5] Anna Maria Coclite. Lecture notes in surface and thin film physics, 2013.

[6] Anna Maria Coclite, Rachel M Howden, David C Borrelli, Christy D Petruczok, Rong Yang, Jose Luis Yagüe, Asli Ugur, Nan Chen, Sunghwan Lee, Won Jun Jo, et al. 25th anniversary article: Cvd polymers: A new paradigm for surface modifi cation and device fabrication. *Advanced Materials*, 25(38):5392–5423, 2013.

[7] Dr. Anna Maria Coclite. Projects. `https://www.annacoclite.com/projects/`. Accessed: 21.03.2017.

[8] Jan Dohnt. *46th IFF Spring School 2015: Functional Soft Matter Lecture Notes*. Forschungszentrum Jlich GmbH, 2015.

[9] Karen K Gleason. *CVD Polymers: Fabrication of Organic Surfaces and Devices*. John Wiley & Sons, 2015.

[10] Hans-Ulrich Gremlich. Infrared and raman spectroscopy. *Ullmann's encyclopedia of industrial chemistry*, 2000.

[11] Shunsuke Hirotsu. Softening of bulk modulus and negative poissons ratio near the volume phase transition of polymer gels. *The Journal of chemical physics*, 94(5):3949–3957, 1991.

[12] R Hoogenboom. Temperature-responsive polymers: properties, synthesis and applications. *Smart polymers and their applications. Elsevier, Cambridge*, pages 15–44, 2014.

[13] Kenneth KS Lau and Karen K Gleason. Initiated chemical vapor deposition (icvd) of poly (alkyl acrylates): an experimental study. *Macromolecules*, 39(10):3688–3694, 2006.

[14] Verena Leitgeb. *Optimized Particle Plasmons for Bio-Sensing*. PhD thesis, Karl-Franzens-Universitt Graz, 2015.

[15] Debashish Mukherji, Carlos M Marques, and Kurt Kremer. Polymer collapse in miscible good solvents is a generic phenomenon driven by preferential adsorption. *Nature communications*, 5, 2014.

[16] Yousuke Ono and Toshiyuki Shikata. Hydration and dynamic behavior of poly (n-isopropylacrylamide) s in aqueous solution: A sharp phase transition at the lower critical solution temperature. *Journal of the American Chemical Society*, 128(31):10030–10031, 2006.

[17] Gozde Ozaydin-Ince and Karen K Gleason. Transition between kinetic and mass transfer regimes in the initiated chemical vapor deposition from ethylene glycol diacrylate. *Journal of Vacuum Science & Technology A: Vacuum, Surfaces, and Films*, 27(5):1135–1143, 2009.

[18] Stefano Palagi, Andrew G Mark, Shang Yik Reigh, Kai Melde, Tian Qiu, Hao Zeng, Camilla Parmeggiani, Daniele Martella, Alberto Sanchez-Castillo, Nadia Kapernaum, et al. Structured light enables biomimetic swimming and versatile locomotion of photoresponsive soft microrobots. *Nature materials*, 2016.

[19] Abdon Pena-Francesch, Laura Montero, and Salvador Borros. Tailoring the lcst of thermosensitive hydrogel thin films deposited by icvd. *Langmuir*, 30(24):7162–7167, 2014.

[20] Eriko Sato Matsuo and Toyoichi Tanaka. Kinetics of discontinuous volume–phase transition of gels. *The Journal of chemical physics*, 89(3):1695–1703, 1988.

[21] Katrin Unger, Roland Resel, and Anna Maria Coclite. Dynamic studies on the response to humidity of poly (2-hydroxyethyl methacrylate) hydrogels produced by initiated chemical vapor deposition. *Macromolecular Chemistry and Physics*, 217(21):2372–2379, 2016.